IEEE Access
Multidisciplinary | Rapid Review | Open Access Journal

Received March 23, 2019, accepted April 7, 2019, date of publication April 12, 2019, date of current version April 30, 2019.

Digital Object Identifier 10.1109/ACCESS.2019.2910891

MPC-Based Slip Ratio Control for Electric Vehicle Considering Road Roughness

YAN MA[1,2], JINYANG ZHAO[1], HAIYAN ZHAO[1,2], CHAO LU[3], AND HONG CHEN[1,2], (Member, IEEE)

[1]Department of Control Science and Engineering, Jilin University, Changchun 130022, China
[2]State Key Laboratory of Automotive Simulation and Control, Jilin University, Changchun 130022, China
[3]95979 troops of the Chinese People's Liberation Army, Shenyang 110045, China

Corresponding author: Haiyan Zhao (hyzhao2008@163.com)

This work was supported in part by the National Nature Science Foundation of China under Grant 61790564, in part by the Joint Project of Jilin Province and Jilin University under Grant SXGJSF2017-2-1-1, in part by the China Automobile Industry Innovation and Development Joint Fund under Grant U1664257, in part by the Industrial Innovation Special Funds of Jilin Province under Grant 2018C035-2, and in part by the Graduate Innovation Fund of Jilin University under Grant 419020391355.

ABSTRACT In this paper, a slip ratio controller based on model predictive control (MPC) considering road roughness is proposed for electric vehicle (EV) to improve the driving/braking performance under low adhesion coefficient road. A half vehicle dynamic model is derived in which pitching, wheel rolling, and tire vertical movement is taking into account. The influence of vertical force variation caused by road unevenness and tire load transfer is analyzed to design slip ratio controller. In order to ensure vehicle safety, wheel slip stable zone is considered as time-domain constraints of the nonlinear-MPC. Besides, the motor output torque is limited by the motor maximum torque, which is considered as system time-varying constraints. The control objectives include vehicle safety, good longitudinal acceleration and braking performance, preservation of driver comfort, and lower power consumption. The proposed slip ratio controller is verified on a 13-degree-of-freedom (13DOF) EV model in MATLAB/Simulink. Simulation results of different maneuver on roughness surfaces show the benefits of the controller.

INDEX TERMS Slip ratio control system, driving/braking torque, uneven road, MPC, electric vehicle.

I. INTRODUCTION

In recent years, the environment concerns and energy conservation has stimulated an increasing research trend towards EVs [1]. The EV with four independent in-wheel motors have become engineering-focus because of their unique structure [2]. Compared with traditional internal combustion engine driving vehicles (ICVs), four wheels can be directly actuated by in-wheel motors without any mechanical links [3] [4]. The motors can be operated in traction and braking modes which promote the development of EV slip ratio control (SRC) system. The SRC strategy also be called longitudinal control, such as anti-lock braking system (ABS) or traction control system (TCS), can effectively prevent the vehicle wheels from locking up during braking or traction [5] [6] [7], thereby enhancing the directional stability and safety of the vehicle. However, SRC do not consider the suppression of vertical vibration under uneven road conditions. Longitudinal-vertical coordinated control is carried out for ABS or ESC with continuous damping control (CDC) or active suspension system (ASS) [8] [9]. The longitudinal-vertical force cooperative control in [10] is based on ABS and CDC. In this paper, a 1/4 vehicle model is established, and the active suspension force of the active suspension output is controlled according to the change of the braking torque of each wheel, so as to control the vertical load of each wheel and obtain the maximum braking force under the current conditions. In [11], a 1/2 vehicle model is established based on [10], and proposed a strategy to consider the joint control of anti-lock braking system and active suspension. In this paper, the active suspension control system sacrifices the comfort of the vehicle to achieve the optimal value of the wheel slip ratio and the maximum value of the tire normal reaction force as the control target, so that the controlled system obtains the maximum braking force and improves the vehicle's Braking performance.

The associate editor coordinating the review of this manuscript and approving it for publication was Xiaosong Hu.

In [12], a layered integrated control system based on 1/2 vehicle model is designed. The control system is divided into two layers. The bottom layer is ASS system and ABS system. In [13], the synergistic control of ESC and CDC under different conditions is proposed. ESC and CDC work independently to improve drive/brake performance and comfort, respectively.

There are several control strategies in the longitudinal-vertical control The goals are achieved by employing nonlinear backstepping schemes, whose design procedure consists of two parts to construct the anti-lock braking and active suspension controllers individually in [14]. The coordinated control of ABS and ASS is proposed in [15] [16] using fuzzy logic control theories to improve braking performance. By derived longitudinal and vertical dynamic nonlinear system models, longitudinal-vertical force coordinated control is realized. In [10], two gain-scheduled controllers are synthesized to achieve attitude and yaw performances according to the driving situation. A layered integrated control system based on a 1/2 vehicle model is designed in [17] to divide the control system into two layers. The bottom layer is the ASS system and the ABS system. The upper layer is the coordinated controller. Through the subsystem controllers, the two subsystems on the bottom layer are coordinated controlled. Subsystem controller applies fuzzy logic algorithm and pitch movement of the vehicle body is taken into account in [11] to control the driving posture of the vehicle. A new type ABS is developed based on full-time feedback control algorithm in [18]. Model predictive controller-based multi-model control system (MPC-MMCS) is proposed to solve the longitudinal stability problem in [19]. However, there are less research on longitudinal-vertical control based on passive suspension under consideration of low adhesion coefficient on uneven road surface. Because the vehicle is easy to slip on a surface with low adhesion coefficient, coupled with the impact of uneven road surface, it will have a great impact on the performance of the vehicle. It is usually required to compensate the vertical force of the active suspension to increase the vertical force, a larger driving force or braking force can be provided. When an electric vehicle equipped with an active suspension is driven, the motor vibration at the vehicle suspension is an important factor affecting the ride comfort, and the presence of multiple motors increases the cost of the electric vehicle. So passive suspension is used in this paper to increase the difficulty of controller design.

During the design process, we considered the vertical load change of the tire under uneven road conditions and considered the physical saturation constraints of the motor. The problems solved by the nonlinear model predictive controller proposed in this paper are as follows: (1) The problem of slip is described as the constraint tracking problem (2) When considering the state equation of the control system the effect of uneven road surface is considered, and the vertical direction is suppressed. (3) More importantly, the MPC strategy can effectively handle the existing constraints (Motor saturation hard constraints and slip ratio constraints) and achieve effective vertical control of the vehicle. The simulation results show that the controller can effectively improve the vehicle handling and comfort performance, and slip ratio can be controlled on the road with low coefficient of friction.

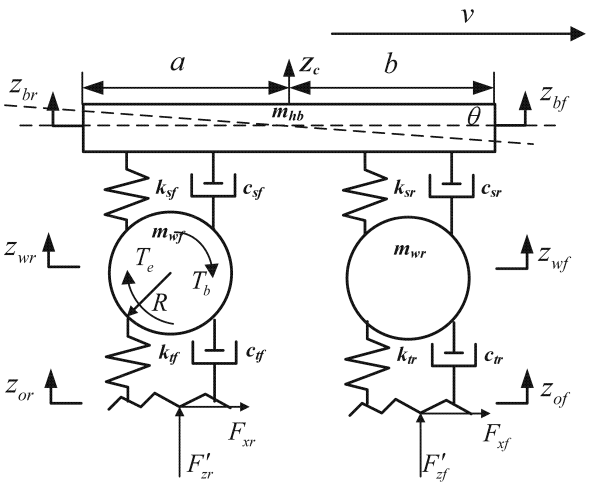

FIGURE 1. Half vehicle model.

The organization of this paper is as follows. In Section 2, a control oriented nonlinear model of EV system is derived and a control problem of slip control is stated in detail. In Section 3, a model predictive control approach for slip ratio control is introduced. Section 4 gives the simulation results to validate the effectiveness of the proposed controller under snow road. Finally the conclusion and future work are summarized in Section 5.

II. VEHICLE DYNAMIC MODEL FOR CONTROLLER DESIGN

A half vehicle dynamic model considering pitching, wheel rolling and tire vertical movement is described in Figure 1 [20], [21].

The vertical vibration displacement of the body at the front suspension and rear suspension is:

$$\ddot{z}_{bf} = \ddot{z}_c - a\ddot{\theta} \tag{1}$$

$$\ddot{z}_{br} = \ddot{z}_c + b\ddot{\theta} \tag{2}$$

where z_{bi} are vertical displacement of front and rear ends of the vehicle body, θ is pitching angle, z_c is vertical displacement at the center of mass of the car.

Referring to the D'Alembert's principle, the dynamic differential equation for the half passive suspension system can be derived. The dynamic equation of the vertical vibration at the center of mass is

$$-m_{hb}\ddot{z}_c + c_{sr}(\dot{z}_{wr} - \dot{z}_{br}) + c_{sf}(\dot{z}_{wf} - \dot{z}_{bf}) + k_{sr}(z_{wr} - z_{br}) + k_{sf}(z_{wf} - z_{bf}) = 0 \tag{3}$$

where $i = f, r$ means the front wheels and rear wheels, m_{hb} is the vehicle mass, m_{wi} are wheel mass, z_{wi} are the vertical displacement of the wheel, c_{si} are damping of the suspension, k_{si} are elasticity coefficient of the suspension.

The dynamic equation of the pitch motion at the center of mass is:

$$I_{hb}\ddot{\theta} + a(k_{sf}(z_{bf} - z_{wf}) + c_{sf}(\dot{z}_{wf} - \dot{z}_{bf})) - b(k_{si}(z_{bi} - z_{wi}) + c_{si}(\dot{z}_{wi} - \dot{z}_{bi})) = 0 \quad (4)$$

Bring equations (1) and (2) into (3):

$$\ddot{z}_{bf} - Ac_{sf}(\dot{z}_{wf} - \dot{z}_{bf}) + Bc_{sr}(\dot{z}_{wr} - \dot{z}_{br}) + Ak_{sf}(z_{wf} - z_{bf}) + Bk_{sr}(z_{wr} - z_{br}) = 0 \quad (5)$$

$$\ddot{z}_{br} - Bc_{sf}(\dot{z}_{wf} - \dot{z}_{bf}) + Cc_{sr}(\dot{z}_{wr} - \dot{z}_{br}) + Bk_{sf}(z_{wf} - z_{bf}) + Ck_{sr}(z_{wr} - z_{br}) = 0 \quad (6)$$

where $A = \left(\frac{1}{m_{hb}} + \frac{a^2}{I_{hb}}\right)$, $B = \left(\frac{1}{m_{hb}} - \frac{ab}{I_{hb}}\right)$, $C = \left(\frac{1}{m_{hb}} + \frac{b^2}{I_{hb}}\right)$.

By analyzing the mechanical relationship between the suspension and the tire, the equation (7) can be derived.

$$F'_{zi} = k_{ti}(z_{wi} - z_{oi}) + c_{ti}(\dot{z}_{wi} - \dot{z}_{oi}) \quad (7)$$

where F'_{zi} are pressure on the tire in the vertical model, z_{oi}, $i = f, r$ are the front and rear wheel excitation.

According to the moment balance, the wheel rotation dynamics can be obtained as

$$J_i\dot{\omega}_i = T_{ei} - T_{bi} - RF_{xi}, i = f, r \quad (8)$$

where J_i are moment of inertia of the wheel, T_{ei} are driving torque, T_{bi} are braking torque, R is wheel effective radius, F_{xi} are longitudinal force.

Accordingly, the dynamics of a half vehicle can be expressed as

$$m_{hb}\dot{v}_x = F_{xf} + F_{xr} - F_{roll} \quad (9)$$

where v_x is longitudinal speed of the vehicle, F_{roll} is rolling friction force.

The vertical loads F_{zi} of four wheels in EVs can be computed as follows. Notice that the pitch of the car body is taken into account.

$$\begin{aligned}
F_{zfl} &= m_{hb}\left(\frac{b}{a+b}g - \frac{h}{a+b}a_x\right)\left(\frac{1}{2} - \frac{ha_y}{t_f g}\right) + \frac{1}{2}F_{zf} \\
F_{zfr} &= m_{hb}\left(\frac{b}{a+b}g - \frac{h}{a+b}a_x\right)\left(\frac{1}{2} + \frac{ha_y}{t_f g}\right) + \frac{1}{2}F_{zf} \\
F_{zrl} &= m_{hb}\left(\frac{b}{a+b}g + \frac{h}{a+b}a_x\right)\left(\frac{1}{2} - \frac{ha_y}{t_r g}\right) + \frac{1}{2}F_{zr} \\
F_{zrr} &= m_{hb}\left(\frac{b}{a+b}g + \frac{h}{a+b}a_x\right)\left(\frac{1}{2} + \frac{ha_y}{t_r g}\right) + \frac{1}{2}F_{zr}
\end{aligned} \quad (10)$$

The tire-load force can be described as

$$F_{xi} = \mu(\lambda) \cdot F_{zi}, i = f, r \quad (11)$$

where

$$\mu(\lambda) = c_1(1 - e^{-c_2\lambda}) - c_3\lambda \quad (12)$$

The values of three variable parameters c_1, c_2, c_3 under five ordinary road surfaces are obtained, as shown in Table 1 [22].

TABLE 1. Parameter values under different pavement conditions.

Road conditions	c_1	c_2	c_3
Dry asphalt	1.2801	23.99	0.52
Wet asphalt	0.857	33.822	0.347
Dry cement	1.1973	25.168	0.5373
Snow	0.1946	94.129	0.0646
Ice	0.05	306	0

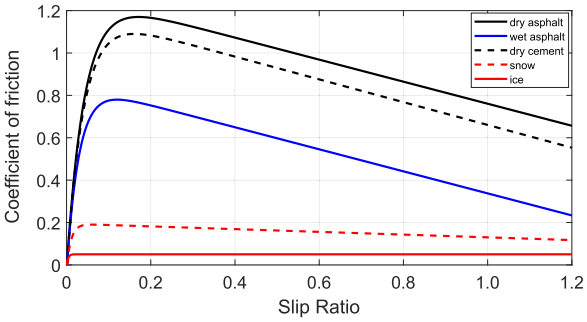

FIGURE 2. Relationship between slip ratio and friction coefficient.

According to the five groups of parameters in Table 1, the five curves shown in Figure 2 can be obtained.

From equations (8) (10) (11), the required wheel drive torque can be obtained:

$$\begin{aligned}
T_{efl} &= \dot{\omega}_{fl} \cdot J + R \cdot \mu(\lambda) \cdot [m_{hb}\left(\frac{b}{a+b}g - \frac{h}{a+b}a_x\right)\left(\frac{1}{2} - \frac{ha_y}{t_f g}\right) + \frac{1}{2}F_{zf}] \\
T_{efr} &= \dot{\omega}_{fr} \cdot J + R \cdot \mu(\lambda) \cdot [m_{hb}\left(\frac{b}{a+b}g - \frac{h}{a+b}a_x\right)\left(\frac{1}{2} + \frac{ha_y}{t_f g}\right) + \frac{1}{2}F_{zf}] \\
T_{erl} &= \dot{\omega}_{rl} \cdot J + R \cdot \mu(\lambda) \cdot [m_{hb}\left(\frac{b}{a+b}g + \frac{h}{a+b}a_x\right)\left(\frac{1}{2} - \frac{ha_y}{t_r g}\right) + \frac{1}{2}F_{zr}] \\
T_{err} &= \dot{\omega}_{fr} \cdot J + R \cdot \mu(\lambda) \cdot [m_{hb}\left(\frac{b}{a+b}g + \frac{h}{a+b}a_x\right)\left(\frac{1}{2} + \frac{ha_y}{t_r g}\right) + \frac{1}{2}F_{zr}]
\end{aligned} \quad (13)$$

Taking the acceleration process as an example and the equation based on the slip ratio can be calculated:

$$\lambda = \frac{\omega R - v_x}{\omega R} \quad (14)$$

Combining equations (13) (14):

$$\dot{\lambda} = \frac{(1-\lambda)[T_i - R\mu(\lambda)Z_i]m_{hb}R}{\omega_i J m_{hb} R} + \frac{[\mu(\lambda)Z_i - F_{roll}]J}{\omega_i J m_{hb} R}, \quad i = f, r \quad (15)$$

The vertical vibration model and longitudinal dynamic model are derived considering the unevenness of the road surface. The vertical forces are obtained by adding the vertical forces in the two models. At the same time, the optimal conditions for snow conditions are obtained through the friction coefficient-slip curve. The slip ratio, combined with tire model, can finally be related to the vertical force. In the

other word, the state equation of the slip ratio related to the road roughness. Next, the control system will be designed based on this state equation.

III. LONGITUDINAL-VERTICAL CONTROLLER DESIGN

In this section, the longitudinal-vertical controller is mainly designed. The general idea is shown in Figure 3. The longitudinal-vertical controller in this paper does not only consider the road surface roughness during modeling, but also considers the road surface roughness when designing the NMPC controller, which is reflected in the equations of state and constraints.

Based on the 1/2 model design controller, the vertical force, the optimal slip ratio and the current time slip ratio are input into the controller. The controller outputs the hub motor demand value, and detects the wheel speed and the vehicle speed input to the slip ratio calculator to calculate the current time slip ratio.

According to the vehicle model analysis, the dynamic equation with the longitudinal slip ratio is adopted as the state variables. The state space equation (16) can be obtained.

$$\begin{aligned}\dot{x}_e &= \frac{T_i - R\mu(x_i)F_{zi}}{\omega_i J_i}(1-x_i) - \frac{\sum_{i=f,r}\mu(x_i)F_{zi} - F_{roll}}{m\omega_i R}\\ \dot{x}_b &= \frac{T_i - R\mu(x_i)F_{zi}}{v_x J_i}R - (1+x_i)\frac{\sum_{i=f,r}\mu(x_i)F_{zi} - F_{roll}}{mv_x}\end{aligned} \tag{16}$$

where $x = [\lambda_f, \lambda_r]^T$ is the state variable, represents the slip ratio of the front and rear wheels, $u = [T_{ef}, T_{er}]^T$ is the input of the system, $y = [\lambda_f, \lambda_r]^T$ represents the slip ratio of the front and rear wheels, is the output of the system.

In order to use the computer to solve the optimization control problem, the system state equation is discretized by numerical calculation method, as shown in equation (17).

$$\begin{aligned}x(k+1) &= f^k(x(k), u(k)) \cdot \Delta t + x(k),\\ y(k) &= C \cdot x(k)\end{aligned} \tag{17}$$

where f^k is the rate of change of the state variable of the controlled system at the time, Δt is the sampling step, $C = [1, 1]$ is the output matrix.

Then the equation (18) is given.

$$\begin{aligned}x_f(k+1) &= [\frac{T_i - R\mu(x(k))Z_i}{\omega_i J_i}(1-x(k))\\ &\quad -\frac{\sum_{i=f,r}\mu(x(k))Z_i - F_{roll}}{m\omega_i R}]\Delta t + x(k)\\ x_r(k+1) &= [\frac{T_i - R\mu(x(k))Z_i}{v_x J_i}R\\ &\quad -(1+x(k))\frac{\sum_{i=f,r}\mu(x(k))Z_i - F_{roll}}{mv_x}]\Delta t + x(k)\\ y(k) &= C \cdot x(k).\end{aligned} \tag{18}$$

This article defines c the control time domain and defines p the prediction time domain. At the k sampling point, the output of the slip ratio control system $U(k)$ and the predicted system $Y(k)$ output sequence are shown below.

$$U(k) = \begin{bmatrix} u(k|k) \\ u(k+1|k) \\ \vdots \\ u(k+c-1|k) \end{bmatrix} Y(k) = \begin{bmatrix} y(k+1|k) \\ y(k+2|k) \\ \vdots \\ y(k+p|k) \end{bmatrix} \tag{19}$$

$R(k)$ is the reference value output by the controlled system, the reference value output in this paper is the optimal value of each tire slip ratio. It is related to the road surface condition. Under the condition of the road surface condition, the slip ratio of the tire is a fixed value. Equation (12) is calculated, so there are $R(k) = [\lambda_{qf}, \lambda_{qr}]^T$.

At the k sampling time, $y(k)$ is the initial value predicted by the control system, $y(k|k) = y(k)$. The updated equations for predicting state variables and predicted outputs of the controlled system are as shown in equations (20) and (21). The state variables and input of the controlled system will be updated according to the current state variable values and system input calculations. The first item of the derived control sequence will be used as the system input to act on the next moment and combined with the controlled system at the next moment. The output solves the optimization problem, so that the rolling optimization of the control sequence is achieved repeatedly, and the state of the future moment is solved.

$$\begin{aligned}x(k+i|k) &= f^k(x(k+i-1|k), u(k+i-1|k)) \cdot \Delta t\\ &\quad +x(k+i-1|k), \quad 1 \le i \le c\end{aligned} \tag{20}$$

$$\begin{aligned}y(k+i|k) &= C(f^k(x(k+i-1|k), u(k+i-1|k)) \cdot \Delta t\\ &\quad +x(k+i-1|k)), \quad 1 \le i \le p\end{aligned} \tag{21}$$

In order to precisely control the slip ratio of each wheel, this section carries out the design of the objective function of the multiple-input and multiple-output slip ratio control system based on the analysis of the control requirements to obtain the three-point control objectives. Based on the control objectives described above, the cost function of the slip rate controller is divided into four parts. The details are as follows.

1. During the running of the vehicle, the tire should provide as long as possible longitudinal force for the vehicle to obtain good acceleration performance and braking performance. Therefore, the slip ratio of the wheel needs to be as large as possible in the stable interval. At the same time, each tire slip ratio is controlled by an objective function in order to be consistent with the rule that the smaller the total objective function value is better.

$$\begin{aligned}J_1 &= \sum_{i=1}^{p}\frac{1}{y(k+i|k)^2 + \delta^2} \cdot Q\\ &= \sum_{i=1}^{p}\left[\frac{1}{\lambda_f(k+i|k)^2+\delta^2} + \frac{1}{\lambda_r(k+i|k)^2+\delta^2}\right] \cdot Q\end{aligned} \tag{22}$$

where y denotes the slip ratio of front and rear wheel Q is a weighted matrix and is used to adjust the weight of the item. When the vehicle starts, the tire slip rate is 0, then equation (20) will appear infinity, this is the controller should not appear, in order to prevent infinity, adding a minimum

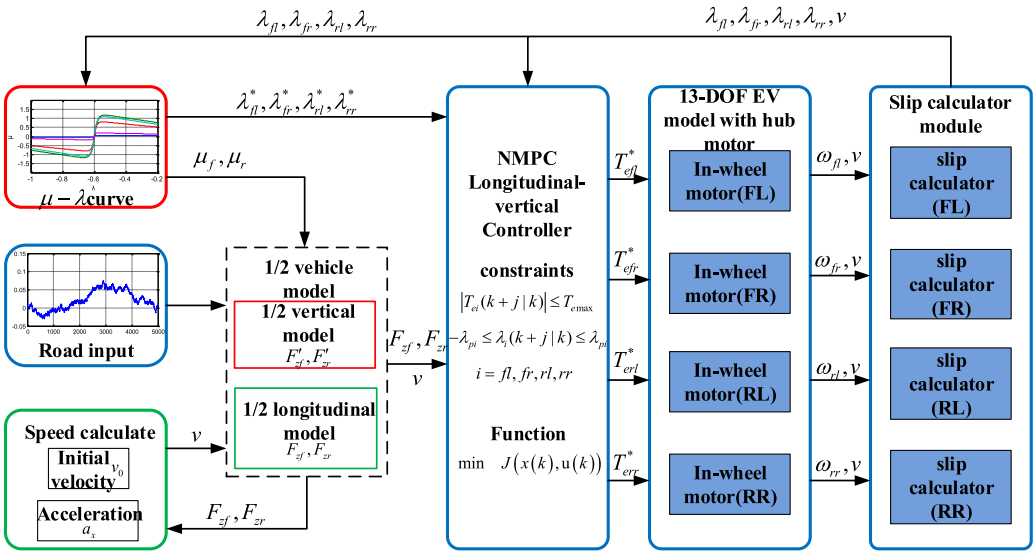

FIGURE 3. Overall structure of longitudinal-vertical control algorithm.

constant δ in the objective function to prevent the denominator of the objective function is zero, after a large number of experiments, $\delta = 0.0001$ in this paper.

2. Considering that in the actual driving process of the vehicle, if the longitudinal force of each wheel reaches the maximum, the transverse force of the vehicle may be too small and the lateral stability may be lost. Therefore, adding the objective function J_1, together with the objective function J_2, enables the vehicle to obtain a large longitudinal force while also ensuring lateral balance.

$$\begin{aligned} J_2 &= \sum_{i=1}^{p} \|y(k+i|k) - r(k+i)\|^2{}_S \\ &= \sum_{i=1}^{p} [S_1 \cdot \left(\lambda_f(k+i|k) - r(k+i)\right)^2 \\ &\quad + S_r \cdot (\lambda_r(k+i|k) - r(k+i))^2] \end{aligned} \tag{23}$$

where $r\,(k+i)$ represents the optimal value of the longitudinal slip ratio of the wheel and the value of this variable is determined by the road surface condition.

3. In order to save the energy of the electric vehicle, on the basis of meeting the performance requirements, the output torque of each wheel should be reduced as much as possible, that is, the smaller the square of the output torque of the wheel, the better. This goal is achieved by adding an objective function J_3.

$$\begin{aligned} J_3 &= \sum_{i=0}^{c-1} \|u(k+i|k)\|^2{}_R \\ &= \sum_{i=0}^{c-1} [R_1 \left(T_f(k+i|k)^2\right) \\ &\quad + R_2 \left(T_r(k+i|k)^2\right)] \end{aligned} \tag{24}$$

4. If there is a large amount of vibration in the acceleration and braking process of the vehicle, it will affect the comfort of the driver, and even affect the operation of the driver, and there are potential safety hazards. In order to avoid this hidden danger, it is required that under the premise of satisfying vehicle performance, the smaller the change rate of each wheel torque is, the better is to ensure the acceleration of the vehicle or the smoothing of the braking by reducing the square sum of the wheel torque change rate. Therefore, the rate of change of the wheel torque is adjusted by adding an objective function J_4.

$$\begin{aligned} J_4 &= \sum_{i=0}^{c-1} \|\Delta u(k+i|k)\|^2{}_P \\ &= \sum_{i=0}^{c-1} [P_1 \left(\Delta T_f(k+i|k)^2\right) \\ &\quad + P_2 \left(\Delta T_r(k+i|k)^2\right)] \end{aligned} \tag{25}$$

Considering the above objective function synthetically and combining all the objective functions in the form of addition as an expression, the overall objective function of the slip ratio control system of the electric vehicle is formed, as shown in equation (26). Equation (27) and (28) is the system constraint of the slip ratio control system. Equation (27)indicates that the output torque of the hub motor cannot be infinite, so the actual torque must be limited to the range of the maximum torque that the hub motor can provide. Inside, this constraint is a hard linear constraint. The equation (27)is used to constrain the longitudinal slip ratio of each tire so that the slip ratio of each wheel is controlled in a stable interval to ensure the acceleration and braking performance of the

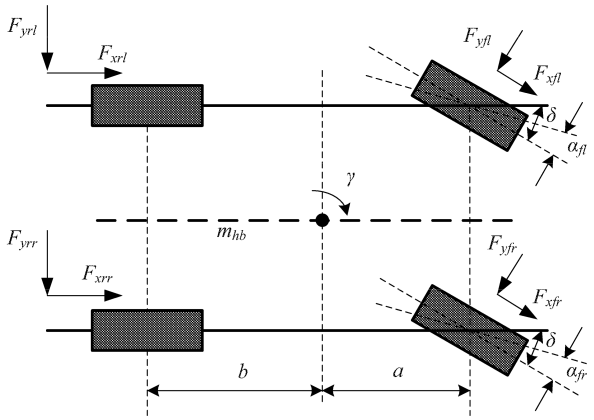

FIGURE 4. 13-DOF vehicle model.

vehicle. The constraint is a nonlinear constraint.

$$\begin{aligned}\min\ J(x(k), U(k)) &= J_1 + J_2 + J_3 + J_4 \\ &= \sum_{i=1}^{p} \frac{1}{y(k+i|k)^2 + \delta^2} \cdot Q \\ &+ \sum_{i=1}^{p} \|y(k+i|k) - r(k+i)\|^2 \cdot S \\ &+ \sum_{i=0}^{c-1} \|u(k+i|k)\|^2 \cdot R \\ &+ \sum_{i=0}^{c-1} \|\Delta u(k+i|k)\|^2 \cdot P. \qquad (26)\end{aligned}$$

$$s.t\ \ |T_{ei}(k+j|k)| \le T_{e\max}, j = 0, 1, \ldots, c-1; \qquad (27)$$

$$-\lambda_{pi} \le \lambda_i(k+j|k) \le \lambda_{pi}, j = 1, \ldots, p. \qquad (28)$$

IV. SIMULATION AND ANALYSIS

The vehicle model used in this study is shown in Figure 4. It is a 13-DOF vehicle model for lateral longitudinal and vertical dynamics, which also takes into account the nonlinearities between vehicle body dynamics and tire forces. Degrees of freedom associated with the model are the rotation of the four wheels, the vertical movement of the four wheels, and the longitudinal and lateral movement of the vehicle, and the pitch, roll and yaw of the vehicle body.

The effectiveness and control performance of the above-designed EV slip ratio control system is verified offline under the Matlab/Simulink. In this paper, a 13-DOF four-wheel hub motor-driven EV model is built in Simulink, which can largely approximate the dynamic characteristics of the real vehicle, and is used to verify the effectiveness of the slip ratio control system on the actual vehicle. The slip ratio controller's objectives are as follows:

(1) The slip ratio is controlled in a stable interval and is close to the optimal value to ensure the acceleration performance and braking performance of the vehicle and improve the vehicle's manipulation.

(2) Under the premise of guaranteeing vehicle performance requirements, try to reduce the magnitude of torque and the magnitude of torque change to save energy and ensure driver's comfort.

TABLE 2. Main parameters of the vehicle model.

Parameter	Symbol	Value
Mass of the half-car	m	$663.5kg$
Moment of inertia of wheels	J	$1kg \cdot m^2$
Rolling radius of the tire	R	$0.291m$
Distance from centroid to front axle	a	$1.2m$
Distance from centroid to rear axle	b	$1.48m$
Height of the vehicle centroid	h	$0.574m$
Stiffness of the tires	k_{tf}, k_{tr}	$220000N/m$
Damping of the tires	c_{tf}, c_{tr}	$100N/(m/s)$
Stiffness of the front suspension	k_{sf}	$24000N/m$
Stiffness of the rear suspension	k_{sr}	$26000N/m$
Damping of the front suspension	c_{sf}	$3900N/(m/s)$
Damping of the rear suspension	c_{sr}	$4300N/(m/s)$

The slip ratio control system must ensure the braking force and driving force of the vehicle to improve the safety and maneuverability of the vehicle even under uneven road conditions. Therefore, this subject chooses to use snow uneven pavement as the external environment. The excitation of the tires on an uneven road surface is a vertical displacement of up to 0.08m and a minimum of -0.03m generated by white noise superposition.

The weighting matrix in the objective function selects the appropriate values Q, S, R, P through a large number of experiments. The prediction time domain P should be greater than or equal to the control time domain C. The greater the value of the two, the more accurate the control result obtained, but the calculation amount of the control system will also increase accordingly. After repeated experiments, the prediction time domain and the control time domain are all selected to be 3, so that the control performance can be satisfied and the control system calculation amount is controlled within an acceptable range. Since the vehicle speed during the simulation is small and the air resistance is very small, air resistance is ignored. The rolling resistance of the vehicle is $F_{roll} = 0.01mg$. To ensure the real-time performance of the model predictive control, the simulation sampling time is set to 1ms. The main parameters of electric vehicles are shown in Table 2. The snow-covered road surface is achieved by selecting corresponding fixed-value coefficients for the tire model. According to Table 1, the three selected coefficients are $c_1 = 0.1946, c_2 = 94.129, c_3 = 0.0646$. The effectiveness of the slip ratio control system is verified through three conditions: starting, driving and braking. These three conditions are typical conditions for verifying the longitudinal mechanical properties of the vehicle. Each condition is divided into no load. For people and five people with full load, the average weight of each person is calculated as $60kg$.

A. ACCELERATING CONDITIONS BASED ON UNEVEN SNOW COVER

In the accelerating conditions, the initial speed of the vehicle is 40km/h, and the road surface conditions are the snow-covered uneven road surface mentioned above. At this time, the best slip ratio of the tire is 0.06, and the maximum

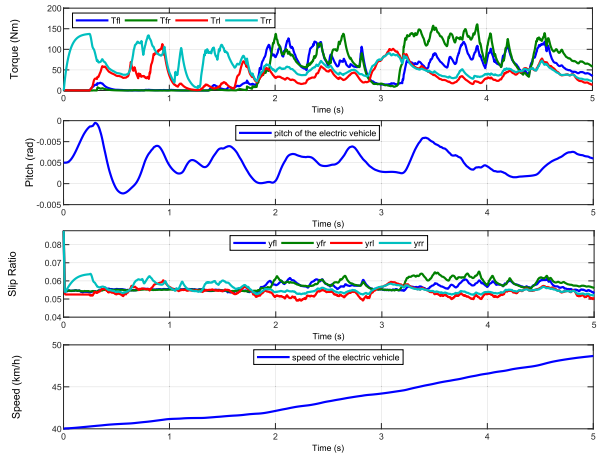

FIGURE 5. Accelerating conditions for no-load vehicles under snow covered roads.

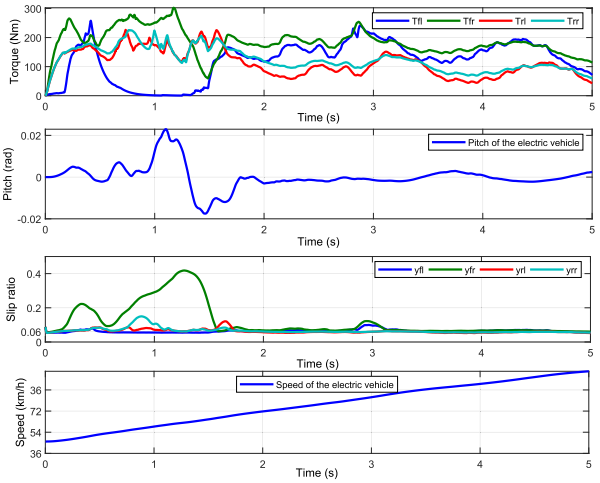

FIGURE 6. Accelerating conditions under full load on snow under uneven snow conditions.

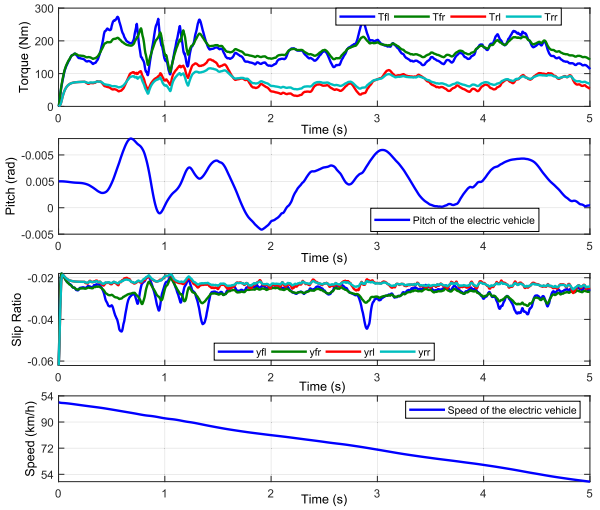

FIGURE 7. Braking conditions under no-load conditions on snow covered roads.

tire-road friction coefficient is 0.19. The vehicle accelerates along a straight line. In the simulation model of a four-wheel hub-driven electric vehicle, the number of steering angles of the two front wheels is set to 0 degrees.

(1) The vehicle is empty

Under this operating condition, the EV will start along a straight line and accelerate, thus obtaining the simulation results of the starting conditions of the vehicle under snow-covered uneven road conditions, as shown in Figure 5.

It can be seen from Figure 5the speed curve that the vehicle accelerates from 40km/h to 50km/h within 5s. Since the vehicle is on the snow-covered road, the vehicle needs to continuously control the torque to ensure that the vehicle does not slip. When the vehicle starts to accelerate, the slip ratio reaches 0.1 to provide a large driving force from the slip ratio curve. But slip ratio quickly converges to an optimum value of 0.06, which ensures the driving performance of the vehicle. Through the curve of the vehicle's pitch angle, the vehicle's pitch angle changes from -0.005 to 0.005 rad to ensure the comfort of the vehicle.

(2) The vehicle is fully loaded with 5 people

In the case of five people, the total mass of the vehicle is increased from 1360 kg without load to 1660 kg. The external road conditions are the same as the no-load conditions. The simulation results are shown in Figure 6.

It can be seen from the speed curve that the vehicle accelerates from 40km/h to 63km/h within 5s. The vehicle torque is about 200Nm. Compared with Figure 5, the vehicle torque becomes larger, which is caused by the increase of the vehicle load. It can be seen from the slip ratio curve that the wheel slip ratio reaches 0.4 in about 1.3s, and the wheel slips. Compared with torque shows that the front wheel torque decreases rapidly and the slip ratio tends to be stable. The wheel slip ratio is around the optimal slip ratio 0.06 after 1.5s. The safety and driveability of the vehicle are guaranteed. Compared witch the pitch angle curve, it can be seen that the pitch angle of the wheel also produces a jitter, but the pitch angle is always maintained between -0.02 and 0.02 rad, which ensures the comfort of the vehicle.

Through two experiments, it can be seen that, the vehicle can guarantee a good driving performance on the snow-covered road, and the controller is effective.

B. BRAKING CONDITIONS BASED ON UNEVEN SNOW COVER

In the braking condition, the initial speed of the vehicle is 80km/h, and the road surface condition is also the snow-covered uneven surface. The optimal slip ratio of the wheel is -0.06, corresponding to the tire and the road surface. The maximum friction coefficient is 0.19, and the steering angle of the two front wheels is set to 0 degrees.

(1) Empty Vehicle

The simulation results of the EV's no-load brake condition are shown in Figure 7.

Through the speed curve, it can be seen that the speed of the vehicle is decelerated from 85km/h to 63km/h within 5s. During the emergency braking process, the vehicle tire load is transferred from the rear wheel to the front wheel, so the

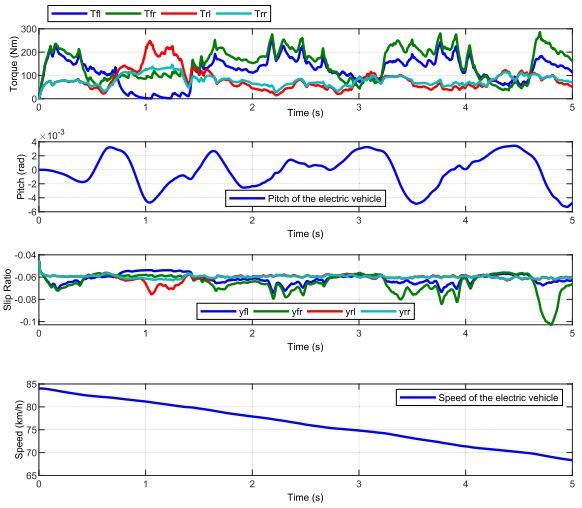

FIGURE 8. Braking conditions under full load of snow under uneven snow conditions.

driving torque of the front wheel is about 200Nm. The rear wheel drive torque is about 100Nm. The slip ratio is kept near 0.03, which ensures the safety performance of the vehicle and the braking performance. The vehicle's pitch angle changes between -0.005 to 0.005 rad, which ensures the comfort of the vehicle.

(2) The vehicle is fully loaded with 5 people

The simulation results under full load of the vehicle are shown in Figure 8. Compared with the braking situation under no-load condition Figure 7, the braking torque of the vehicle is slightly larger and faster.This is because the load is getting bigger, and the wheels are more sensitive to the road. The slip ratio is maintained near 0.06 optimal slip ratio during the entire braking process.The vehicle speed is reduced from 85km/h to 70km/h, which ensures the braking performance of the vehicle. The vehicle's pitch angle changes between-0.005 to 0.005 rad, which ensures the comfort of the vehicle.

The experimental results under the braking conditions under snow cover and uneven road conditions, the slip ratio control system designed in this paper can avoid excessive slippage of tires under no-load or full-load conditions, thereby improving vehicle safety and acceleration performance. At the same time, it guarantees less energy consumption and also ensures driver's comfort.

V. CONCLUSION

The problem of slip ratio control of four-wheel hub-drive EVs on uneven adhesion surfaces is solved. The system fully utilize the wheel load to provide more reasonable driving force or braking force for electric vehicles and improve the performance of EV's safety and motivation. The impact of uneven road surface on electric vehicles is taken in account in the modeling process. By considering the safety constraints, the slip controller designed by the hard-constrained motor suppresses the vertical load changes caused by uneven road surfaces, while providing greater longitudinal forces. The designed controller is verified on the 13DOF model. The results show that the control of the slip ratio is in the stable range. It provides a large drive braking force with a small range of pitch angle and ensures comfortable. In the future, the integrated control of longitudinal lateral and vertical will be taken into account. Then, the hardware-in-the-loop experiment of FPGA will be added.

REFERENCES

[1] Y. Hori, Y. Toyoda, and Y. Tsuruoka, "Traction control of electric vehicle: Basic experimental results using the test EV 'UOT electric march," *IEEE Trans. Ind. Appl.*, vol. 34, no. 5, pp. 1131–1138, Sep./Oct. 1998.

[2] N. Mutoh, "Driving and braking torque distribution methods for front- and rear-wheel-independent drive-type electric vehicles on roads with low friction coefficient," *IEEE Trans. Ind. Electron.*, vol. 59, no. 10, pp. 3919–3933, Oct. 2012.

[3] H. Sado, S. Sakai, and Y. Hori, "Road condition estimation for traction control in electric vehicle" in *Proc. IEEE Int. Symp. Ind. Electron.*, vol. 2, pp. 973–978, Jul. 1999.

[4] W.-Y. Wang, I.-H. Li, M.-C. Chen, S.-F. Su, and S.-B. Hsu, "Dynamic slip-ratio estimation and control of antilock braking systems using an observer-based direct adaptive fuzzy—Neural controller," *IEEE Trans. Ind. Electron.*, vol. 56, no. 5, pp. 1746–1756, May 2009.

[5] V. Ivanov, D. Savitski, and B. Shyrokau, "A survey of traction control and antilock braking systems of full electric vehicles with individually controlled electric motors," *IEEE Trans. Veh. Technol.*, vol. 64, no. 9, pp. 3878–3896, Sep. 2015.

[6] K. Han, M. Choi, B. Lee, and S. B. Choi, "Development of a traction control system using a special type of sliding mode controller for hybrid 4WD vehicles," *IEEE Trans. Veh. Technol.*, vol. 67, no. 1, pp. 264–274, Jan. 2018.

[7] R. De Castro, R. E. Araújo, and D. Freitas, "Wheel slip control of EVs based on sliding mode technique with conditional integrators," *IEEE Trans. Ind. Electron.*, vol. 60, no. 8, pp. 3256–3271, Aug. 2013.

[8] Y. Cao, L. Zhai, T. Sun, and H. Gu, "Straight running stability control based on optimal torque distribution for a four in-wheel motor drive electric vehicle," *Energy Procedia*, vol. 105, pp. 2825–2830, May 2017.

[9] J. Yoon, W. Cho, B. Koo, and K. Yi, "Unified chassis control for rollover prevention and lateral stability," *IEEE Trans. Veh. Technol.*, vol. 58, no. 2, pp. 596–609, Feb. 2009.

[10] C. Poussot-Vassal, O. Sename, L. Dugard, P. Gáspár, Z. Szabó, and J. Bokor, "Attitude and handling improvements through gain-scheduled suspensions and brakes control," *Control Eng. Pract.*, vol. 19, no. 3, pp. 252–263, 2011.

[11] A. Alleyne, "Improved vehicle performance using combined suspension and braking forces," *Vehicle Syst. Dyn.*, vol. 27, no. 4, pp. 235–265, 1997.

[12] W.-E. Ting and J.-S. Lin, "Nonlinear control design of anti-lock braking systems combined with active suspensions," in *Proc. 5th Asian Control Conf.*, vol. 1, Jul. 2004, pp. 611–616.

[13] C. Chu, and W. Chen, "Vehicle chassis system based on layered coordinated control," *Chin. J. Mech. Eng.*, vol. 44, no. 2, p. 152, 2008.

[14] K. Y. Wang *et al.*, "Research on vehicle chassis integrated control technology based on coordination strategy," *Appl. Mech. Mater.*, vols. 249–250, pp. 667–671, 2012.

[15] M. M. S. Kaldas, R. Henze, and F. Küçükay, "Improvement of heavy vehicles ride and braking P erformance via combined suspension and braking systems control," *SAE Int. J. Mater. Manuf.*, vol. 4, no. 1, pp. 535–552, 2011.

[16] J. Shao, L. Zheng, Y. N. Li, J. S. Wei, and M. G. Luo, "The integrated control of anti-lock braking system and active suspension in vehicle," in *Proc. 4th Int. Conf. Fuzzy Syst. Knowl. Discovery*, vol. 4, Aug. 2007, pp. 519–523.

[17] J. Yoon, W. Cho, K. Yi, and B. Koo, "Unified chassis control for vehicle rollover prevention," *IFAC Proc. Volumes*, vol. 41, no. 2, pp. 5682–5687, 2008.

[18] S. B. Choi, "Antilock brake system with a continuous wheel slip control to maximize the braking performance and the ride quality," *IEEE Trans. Control Syst. Technol.*, vol. 16, no. 5, pp. 996–1003, Sep. 2008.

[19] K. Shi, X. Yuan, and L. Liu, "Model predictive controller-based multi-model control system for longitudinal stability of distributed drive electric vehicle," *ISA Trans.*, vol. 72, pp. 44–55, Jan. 2018.

[20] X. Tang, D. Zhang, T. Liu, A. Khajepour, H. Yu, and H. Wang, "Research on the energy control of a dual-motor hybrid vehicle during engine start-stop process," *Energy*, vol. 166, pp. 1181–1193, Jan. 2019.
[21] X. Tang, X. Hu, W. Yang, and H. Yu, "Novel torsional vibration modeling and assessment of a power-split hybrid electric vehicle equipped with a dual-mass flywheel," *IEEE Trans. Veh. Technol.*, vol. 67, no. 3, pp. 1990–2000, Mar. 2018.
[22] J. Zhang, W. Sun, and H. Jing, "Nonlinear robust control of antilock braking systems assisted by active suspensions for automobile," *IEEE Trans. Control Syst. Technol.*, to be published.

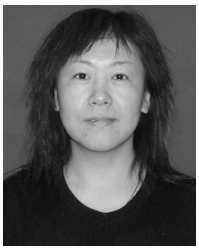

YAN MA received the B.S. degree in automation from the Department of Automation, Harbin Engineering University, Harbin, China, in 1992, and the M.S. degree in control theory and control engineering and the Ph.D. degree in communication and information system from the Department of Control Science and Engineering, Jilin University, Changchun, China, in 1995 and 2006, respectively. In 1995, she joined the former Jilin University of Technology. She was a Postdoctorate at Poly U, Hong Kong. Since 2009, she has been a Professor with Jilin University. Her current research interests include nonlinear estimation methods, applications in power management systems of electric vehicles, and robust filter methods, such as state of charge (SOC) estimation, state of health estimation, state of power estimation, and battery equalization.

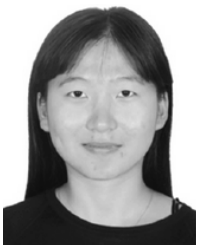

JINYANG ZHAO received the B.S. degree in automation from Jilin University, Changchun, China, in 2017, where she is currently pursuing the master's degree in control theory and control engineering with the Department of Control Science and Engineering. Her current research focuses on the chassis control of the electric vehicle.

HAIYAN ZHAO received the B.S. degree in automation, and the M.S. and Ph.D. degrees in control theory and control engineering from Jilin University, Changchun, China, in 1998, 2004, and 2007, respectively. Since 2016, she has been an Associate Professor with Jilin University. Her current research interests include model predictive control, vehicle stability control, and state estimation of electric vehicles.

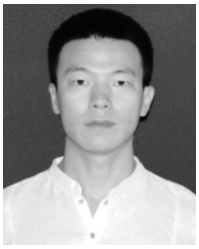

CHAO LU received the B.S. degree in simulation engineering from the School of Mechatronics Engineering and Automation, National University of Defense Technology, Changsha, Hunan, and the M.S. degree in control engineering from the School of Communication Engineering, Jilin University, Changchun, Jilin, 2018. He is currently with the 95979 troops of the Chinese People's Liberation Army.

HONG CHEN received the B.S. and M.S. degrees in process control from Zhejiang University, Zhejiang, China, in 1983 and 1986, respectively, and the Ph.D. degree in system dynamics and control engineering from the University of Stuttgart, Stuttgart, Germany, in 1997. Since 1999, she has been a Professor with Jilin University, Changchun, China, where she currently serves as a Tang Aoqing Professor and as the Director of the State Key Laboratory of Automotive Simulation and Control. Her current research interests include model predictive control, optimal and robust control, nonlinear control, and applications in mechatronic systems focusing on automotive systems.